Anelasticity and viscosity of partially molten rock analogue: Toward seismic detection of small quantities of melt

Christine McCarthy[1,2] and Yasuko Takei[1]

[1] Anelasticity and diffusion creep viscosity of partially molten rock analogue were measured experimentally at various melt fractions (0.0025–0.04). The presence of even a small quantity of melt phase causes a significant increase in attenuation and dispersion, and decrease in viscosity (melt effect). Similar changes are additionally caused by the presence of a secondary solid component (chemical effect). The similitude that was observed in the anelasticity of melt-free systems when scaled by the Maxwell frequency for temperature and grain size effects was observed, too, in that of melt-bearing systems when scaled by the Maxwell frequency for melt and chemical effects. The combined melt and chemical effects on anelasticity offer a potential means of identifying small quantities of melt with seismic velocity perturbations. **Citation:** McCarthy, C., and Y. Takei (2011), Anelasticity and viscosity of partially molten rock analogue: Toward seismic detection of small quantities of melt, *Geophys. Res. Lett.*, *38*, L18306, doi:10.1029/2011GL048776.

1. Introduction

[2] The quantitative effect of melt on seismic wave velocity is of fundamental importance to consider the detectability of melt from seismological methods. The presence of melt has two effects on seismic wave velocity. One is a direct effect due to the contrast in elastic properties between melt and solid, called the poroelastic effect. The other is indirect and attributed to enhanced attenuation and dispersion by melt, called the anelastic effect [e.g., *Karato and Spetzler*, 1990]. Although quantitative assessment of the poroelastic effect has been performed both theoretically and experimentally [e.g., *Mavko*, 1980; *Takei*, 1998, 2000], the anelastic effect has been poorly understood. The anelastic effect is particularly important to consider seismological detection of a small quantity of melt ($\ll$1%), which is expected to exist in the upper mantle [e.g., *Hirschmann*, 2010] but exhibits a very small poroelastic effect. *Jackson et al.* [2004] observed a significant shape change in the attenuation spectrum by melt, whereas *Gribb and Cooper* [2000] did not. Additional experimental work is needed to resolve such discrepancies. In this study, the systematic effects of melt are investigated by using a partially molten rock analogue.

2. Experimental Approach

[3] In a previous study, *McCarthy et al.* [2011], we presented a detailed report of the viscoelastic properties of polycrystalline aggregates of borneol (melting temperature: $T_M = 204.5°C$) and their similarity to those of olivine aggregates. In this study, aggregates of borneol + melt were prepared by partially melting samples made from the borneol($C_{10}H_{18}O$)-diphenylamine((C_6H_5)$_2$NH) binary eutectic system (eutectic temperature: $Te = 43°C$; eutectic composition: 83.3 wt% diphenylamine). This system was selected because it displays an equilibrium microstructure very similar to that of olivine + basalt (dihedral angle = 35° at $T = 47°C$ [*Takei*, 2000]). The system demonstrates a "simple" eutectic reaction in that the solids exhibit no measurable mutual solubility [*Takei*, 2000]. With addition of a specific wt% diphenylamine (W), the melt fraction ϕ just above Te can be accurately controlled as $\phi = W/83.3$. The difference between weight and volume fractions of melt is negligible. High purity borneol is melt-free up to T_M.

[4] Fine powder starting materials of 0.21 – 3.33 wt% diphenylamine, corresponding to melt fractions $0.0025 \leq \phi \leq 0.04$, were prepared by solid-state mixing and ball-milling at low temperature (−40°C). Fully dense cylindrical samples (radius = 15 mm; $55 \leq$ height (mm) ≤ 66) were prepared by pressing the mixed powder in a cylindrical die to 13.9 MPa at room temperature for 48 h. The initial grain size was $d \sim 3~\mu$m, with diphenylamine grains distributed homogenously throughout. Samples were placed between platens and sealed in non-reactive plastic bags to prevent sublimation and/or evaporation at elevated temperature. Details of the sample assembly are given by *Takei et al.* [2011].

[5] Table 1 presents a summary of all binary samples tested in this study and, for comparison, a high purity borneol sample previously reported by *McCarthy et al.* [2011] (sample 15). For simplicity, each sample is referred to here by its melt fraction ϕ at 48°C. The anelasticity and viscosity of these binary samples were measured at $T > Te$ (47.0–48.8°C, hereafter referred to as "suprasolidus temperature") to investigate these properties as functions of melt fraction and also at $T < Te$ (22.2–24.9°C; referred to as "subsolidus temperature") to investigate the solid-state influence of the secondary component. In the anelasticity experiments, we applied a sinusoidally varying uniaxial stress (zero-to-peak amplitude $\sigma_0 \cong 0.014$ MPa), in addition to an offset stress ($\sigma = 0.083 \pm 0.01$ MPa), to measure Young's modulus E and attenuation Q^{-1} over a broad frequency range ($f = 10$–10^{-4} Hz). In the creep experiments, we applied a nominally constant stress ($\sigma \approx 0.083$ MPa), to measure steady-state viscosity η. For each sample, mechanical testing involved three stages. (1) Initial testing was conducted at subsolidus temperature to ensure contact with both platens by creep (as confirmed by modulus measurements). (2) After an anneal at $T = 47°C$ for more than 12 h (to ensure grain growth and textural equilibration), testing at suprasolidus temperature

[1]Earthquake Research Institute, University of Tokyo, Tokyo, Japan.
[2]Now at Lamont-Doherty Earth Observatory, Earth Institute at Columbia University, Palisades, New York, U.S.A.

Table 1. Sample Characteristics at Each Melt Fraction

Melt Fraction ϕ	Thermal History[a] (h)	Grain Size[b] (μm)	Temperature[c] (°C)	Viscosity η (Pa s)
0	sample 15[d]	22.0(0.3)	45.4(±0.1)	5.1×10^{12}
	sample 15[d]	22.0(0.3)	23.7(±0.2)	5.1×10^{13}
0.0025	17.4		47.4(±0.7)	8.0×10^{10}
	24.9	20.5(1.9)	23.2(±0.7)	4.3×10^{12}
0.005	29.5[e]	25.8(2.5)	47.5(±0.6)	1.2×10^{11}
	27.5[e]		23.2(±0.7)	9.6×10^{12}
0.01	17.3		47.4(±0.5)	6.4×10^{10}
	41.2		47.7(±0.6)	7.6×10^{10}
	46.8	25.1(1.8)	24.0(±0.3)	1.1×10^{13}
0.02	19.3		47.8(±0.7)	5.3×10^{10}
	43.8		47.8(±0.7)	6.8×10^{10}
	49.1	26.5(0.2)	23.8(±0.9)	1.2×10^{13}
0.04a	10.7		48.8(±0.8)	2.3×10^{10}
	34.1	29.7(0.7)	24.9(±0.3)	8.8×10^{12}
0.04b	18.8		47.0(±1.0)	3.4×10^{10}
	25.0	24.5(3.4)	NT[f]	NT[f]
	42.5		47.2(±1.1)	5.1×10^{10}
	48.0	28.6(0.9)	22.2(±0.2)	7.2×10^{12}

[a]Duration of suprasolidus temperature anneal.
[b]Error (μm) is given in parentheses.
[c]Error (°C) is given in parentheses.
[d]Detailed thermal history can be found in work by *McCarthy et al.* [2011].
[e]The order of testing was reversed for sample 0.005.
[f]NT means the companion sample was not mechanically tested.

was conducted. In some cases, a second round of testing was performed at this temperature to gauge the effect of further grain growth, if any, during this stage. (3) Finally, after cool down (~3 K/h) and temperature equilibration, testing at subsolidus temperature was again conducted. Each stage consisted of both anelasticity and viscosity testing and lasted between one and three days, with final strain approximately 5%.

[6] Grain growth in the binary system is rapid, even at subsolidus temperature. For this reason, grain size during initial testing at subsolidus temperature could not be constrained and data from stage (1) are excluded. During the suprasolidus temperature annealing of stage (2), very rapid grain growth occurs. However, as is the case with high purity borneol, grain growth becomes extremely slow (relative to the duration of testing) beyond ~22 μm. We found that the rate after a 12 h anneal is sufficiently slow such that tests at suprasolidus and final subsolidus temperatures are conducted at approximately constant grain size. To confirm this, reproducibility was checked between two suprasolidus runs for samples 0.01, 0.02 and 0.04b (Table 1). Also, for sample 0.04b, a small companion sample made of the same powder was used to measure the grain size mid-run without destroying the testing sample. Microstructural examination of this and post-deformation samples was conducted with a confocal light microscope. To closely observe the sample microstructures, post-deformation samples were re-equilibrated at suprasolidus temperature for a few hours and quenched. Sublimation of borneol is faster at grain boundaries and faster still at the interface with quenched melt, thereby etching the microtomed cross-sectional surface and indicating melt even where it is otherwise undetectable. Mean grain size was measured using the line intercept method with a correction factor of 1.5.

[7] For experimental details relating to temperature control, data acquisition, and analysis, see *McCarthy et al.* [2011]. *McCarthy et al.* [2011] present explicit relationships of Young's modulus-type attenuation Q_E^{-1} and uniaxial viscosity η_E (measured in this study), with shear attenuation Q_μ^{-1} and shear viscosity η_μ (measured in torsion experiments), respectively. Q_E^{-1} obtained for the present samples are shown to be almost equal to Q_μ^{-1}, because of the large Poisson's ratio of borneol. In this study, we use Q^{-1} and η (without subscripts) to represent Q_E^{-1} and η_E, respectively.

3. Results

[8] In Figure 1, microstructures of quenched, post-deformation samples demonstrate that melt in this system resides in an interconnected network of triple grain junctions, similar to that of partially molten rocks [e.g., *Cooper and Kohlstedt*, 1984]. Even at $\phi = 0.0025$, small grooves at triple junctions caused by enhanced sublimation indicate the existence of connected melt. No such grooves were observed in high purity samples even after annealing at 60°C [*McCarthy et al.*, 2011]. The final grain sizes were $d = 20.5$–29.7 μm, approximately independent of ϕ (Table 1). The grain size of the companion sample to 0.04b, measured just after the first suprasolidus run, was nearly the same as that of the final, post-deformation sample: less than 16% between 25 and 48 h. In a separate study, grain growth of a $\phi = 0.1$ sample at 47°C was less than 12% between 48 and 250 h (from 21 to 23.5 μm). Further, results from the second suprasolidus runs (samples 0.01, 0.02, and 0.04b) were consistently just slightly smaller in Q^{-1} and slightly larger in η (Table 1) than those from the first runs. These observations validate our treatment of the data here as pertaining to constant grain size. Strain amplitude independence of attenuation and modulus (i.e., linearity) was confirmed by a suite of tests conducted at various stress/strain amplitudes on samples with the highest melt fraction ($\phi = 0.04$b; $\sigma_0 \cong 0.007$ and 0.014 MPa) as well as the lowest ($\phi = 0$; $\sigma_0 \cong 0.0045$–0.077). Also, stress in the creep experiment is within the linear (Newtonian) range [*Takei*, 2001].

[9] Measured anelasticity is shown in Figure 2a. Data are compared to a high purity borneol sample (diamonds with
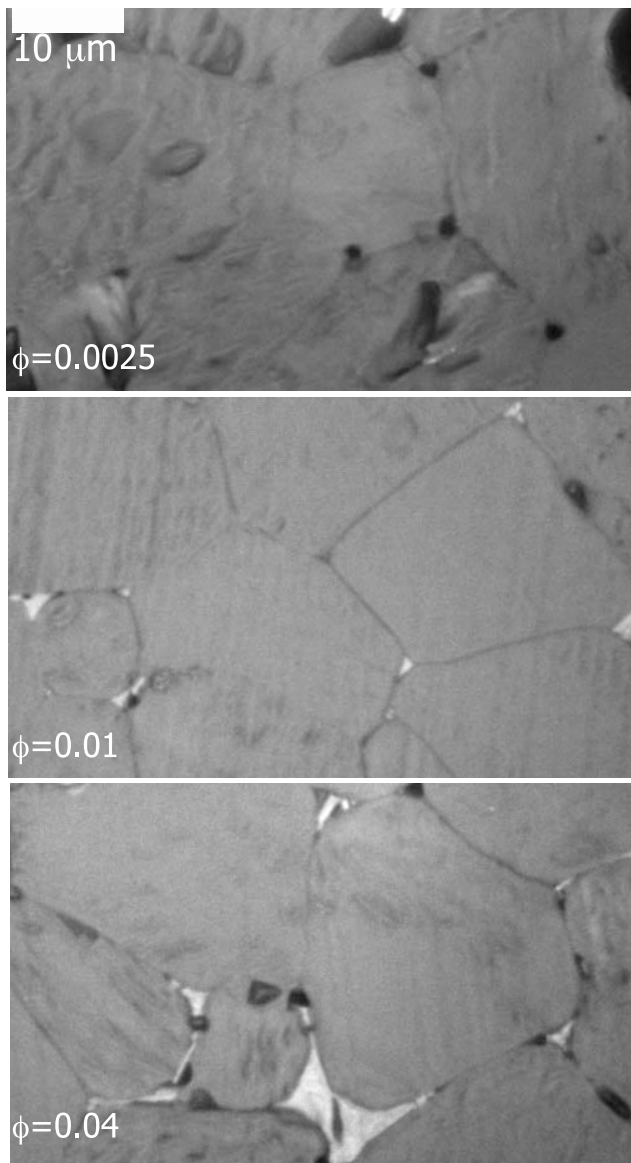
Figure 1. Light microscope images of quenched microstructure of borneol + melt taken post-deformation (all at the same scale). Quenched melt is evident in $\phi = 0.04$ and 0.01 samples as the light phase in triple junctions of grains. In the $\phi = 0.0025$ sample, melt is indicated by tiny holes at triple junctions that form because of preferential sublimation at the melt-grain interface.

dashed line). The suprasolidus data (colored symbols) show significant dispersion and attenuation with increasing melt fraction. The discrepancy between 0.04a and 0.04b is considered to be due to a short annealing time for 0.04a (Table 1), indicating a smaller grain size. The subsolidus data (gray symbols) are almost independent of chemical composition and show considerably larger anelastic relaxation than the high purity borneol sample at similar temperature. Measured viscosities at suprasolidus and subsolidus temperatures for binary samples with various melt fractions are shown in Figure 3 together with data for high purity borneol ($\phi = 0$). Consistent with anelasticity, viscosity was significantly reduced by melt at suprasolidus temperature, and was additionally reduced by the secondary component

even at subsolidus temperature. The high purity borneol data shown in Figures 2 and 3 are highly reproducible [*McCarthy et al.*, 2011]. To demonstrate this, another set of viscosity measurements at $\phi = 0$ is plotted in Figure 3 (squares).

[10] *McCarthy et al.* [2011] observed similar correlation between anelasticity and viscosity and found that normalization of data by the Maxwell frequency $f_M(d, T) = E_U(T)/\eta(d, T)$ (where $E_U(T)$ is the temperature-dependent unrelaxed modulus determined from ultrasonic measurements [*Takei*, 2000]) resulted in collapse of all anelasticity data—regardless of temperature, grain size, or material—onto a single master curve. In this study, we used $E_U(T)$ and measured viscosities for each sample and for each run (Table 1) to calculate the Maxwell frequency f_M, with which we normalize the frequency of anelasticity data (Figure 2b). Modulus data were corrected for both temperature and poroelastic effects. For the poroelastic effect, reduction of E_U by melt was calculated as $E_U (T, \phi)/E_U(T) = 1, 0.973, 0.959, 0.935, 0.893,$ and 0.815 for $\phi = 0, 0.0025, 0.005, 0.01, 0.02,$ and 0.04, respectively, by applying the theoretical model of *Takei* [1998] to dihedral angle 35°, Poisson's ratio 0.37 (borneol [*Takei*, 2000]), and a drained condition of melt. Figure 2b demonstrates that Q^{-1} and corrected E for the binary samples collapse onto single master curves, whereas E prior to the poroelastic correction scatters significantly (inset). There is good agreement between pure and binary samples in the normalized Q^{-1} data, but the normalized E data display a significant deviation.

4. Discussion and Conclusion

[11] In our study, large increases in modulus dispersion and attenuation were observed even with a small quantity of melt (Figure 2a). The successful normalization in Figure 2b demonstrates that the effect of melt on anelastic relaxation is well captured by viscosity. Partial melt viscosity has been derived theoretically in terms of contiguity φ and melt-free viscosity η_0 as $\eta = 0.2\varphi^2\eta_0$ [*Takei and Holtzman*, 2009]. The melt fraction dependence predicted by this model, which uses the semiempirical relationship, $\varphi = 1 - A\phi^{1/2}$ ($A = 2.3$), was shown to be consistent with the relationship $\eta \propto \exp(-\lambda\phi)$ ($\lambda = 30$ [*Hirth and Kohlstedt*, 2003]) known for the diffusion creep viscosity of partially molten rocks. Additionally, the contiguity model predicts an almost discontinuous reduction of η (from η_0 to $0.2\eta_0$) by an extremely small quantity of melt. Our suprasolidus data are consistent with this prediction and can be closely fitted by:

$$\eta = 0.2B\varphi^2\eta_0, \quad (1)$$

with $B = 0.12$ (Figure 3). The additional factor B represents the effect of the secondary component on the creep kinetics (probably through the effect on grain boundary structure and diffusivity), which was not considered in the original model. The existence of this "chemical effect" is supported also by the subsolidus data, which display a significant softening of binary samples roughly consistent with B (Figure 3, gray symbols). A similar two-order-of-magnitude difference in viscosity between melt-free and melt-bearing samples was also reported for the olivine + basalt system [*Faul and Jackson*, 2007].

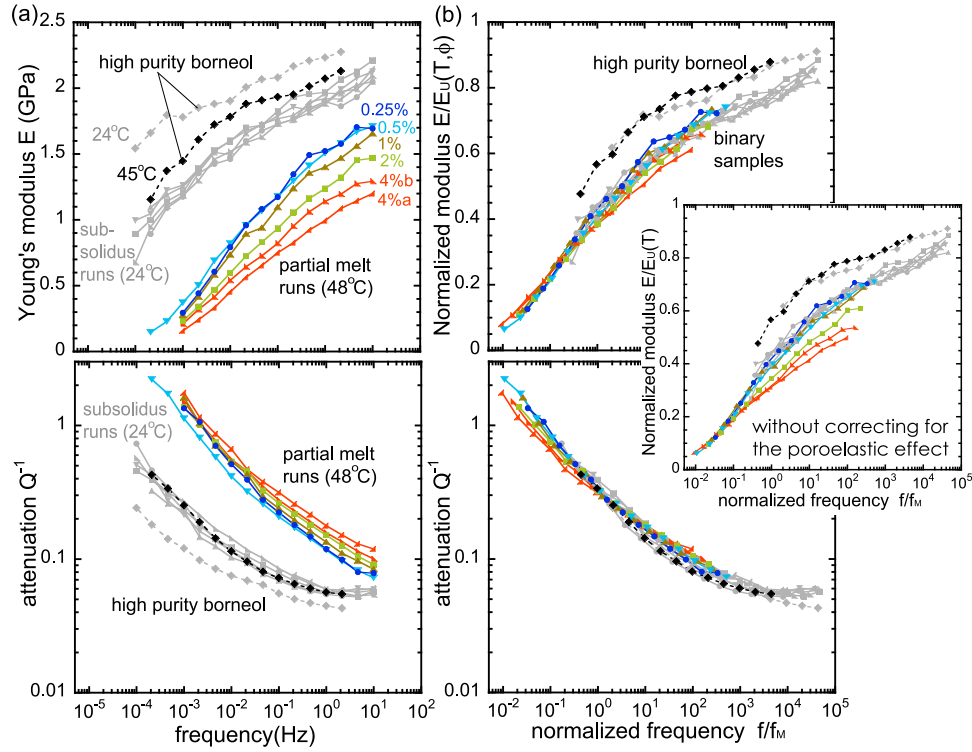[12] Our results show that the similitude applied to the temperature, grain size, and pressure effects [*McCarthy*

Figure 2. (a) Young's modulus E and attenuation Q^{-1} at suprasolidus (48°C; black and colored symbols) and subsolidus (24°C; gray symbols) as functions of frequency f. (b) Normalized modulus $E/E_U(T, \phi)$ as functions of frequency normalized to the Maxwell frequency. Data from the same sample are shown by the same symbol type. For samples 0.01, 0.02, and 0.04b, data from the first suprasolidus run are shown. All data correspond to approximately constant grain size.

et al., 2011] can be further applied to the effects of melt fraction (melt effect) and chemical composition (chemical effect). The extended similitude can be explicitly expressed by the reference time scale τ_r as

$$\tau_r(d, T, P, \phi, c) = \tau_M = J_U(T, P)\eta_0 A(\phi)B(c)\left(\frac{d}{d_r}\right)^m$$
$$\cdot \, e^{-\lambda\phi}e^{\frac{U}{R}\left(\frac{1}{T}-\frac{1}{T_r}\right)}e^{\frac{V}{R}\left(\frac{P}{T}-\frac{P_r}{T_r}\right)}, \qquad (2)$$

where $J_U(T, P)$ is the unrelaxed elastic compliance, $\tau_M = f_M^{-1}$, c is the concentration of the secondary component, $A(\phi = 0) = 1$, $A(\phi \neq 0) = 0.2$, $B(c = 0) = 1$, and $B(c \neq 0) = 0.12$. The large drop of normalized modulus data displayed by the binary samples (Figure 2b), however, means that the chemical effect cannot be fully captured by this scaling. Because normalized Q^{-1} is similar within the experimental frequency range, there must exist a high frequency Q^{-1} anomaly due to the chemical effect, as further suggested by the upward deviation of the binary Q^{-1} data from the pure Q^{-1} data at $f/f_M > 5 \times 10^3$ (Figure 2b).

[13] The universality of the Maxwell frequency scaling demonstrates that the same mechanism, diffusionally accommodated grain boundary sliding, is responsible for attenuation in melt-bearing samples as in melt-free samples [McCarthy et al., 2011]. Partial melt enhanced the mechanism, but did not create a unique relaxation mechanism. Only for the chemical effect was an additional high frequency anomaly in Q^{-1} indicated. This result differs from that of a previous study in which melt-bearing olivine showed a considerable shape change in its Q^{-1} spectrum [Jackson et al., 2004]. The reason for this discrepancy is still

unknown. As discussed in McCarthy et al. [2011], normalized seismic frequency is $f/f_M = 10^{6-9}$, which is not attained by these experiments. Higher frequency data are needed to conclude whether or not the scaling of equation (2) extends into the seismic range.

[14] Can an extremely small amount of melt be detected seismologically? We further consider this question by simply assuming that the scaling in equation (2) applies to seismic waves. Perturbation of shear wave velocity due to the anelastic effect is given by $\Delta \ln V_S = \pi^{-1} Q_s^{-1} \Delta \ln \tau_r$ [e.g., McCarthy et al., 2011, equation (20)]. A significant decrease in η due to an infinitesimal amount of melt causes
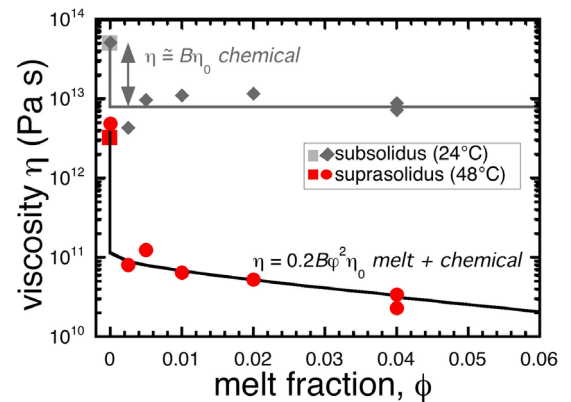

Figure 3. Steady-state viscosity versus melt fraction at suprasolidus (red symbols) and subsolidus (gray symbols). All data correspond to approximately constant grain size.

$\Delta \ln \tau_r = 1.6$ (melt effect, factor A in equation (2)) or $\Delta \ln \tau_r = 3.7$ (melt + chemical effect, factor $A \times B$). Hence, for $Q_S = 80$ (PREM), the estimated velocity perturbation is 0.6% or 1.5%, respectively. A further decrease in V_S might be caused by the high frequency Q^{-1} anomaly. This result indicates the possibility of detecting miniscule quantities of melt, even though poroelastic effects are very small.

References

Cooper, R. F., and D. L. Kohlstedt (1984), Solution-precipitation enhanced diffusional creep of partially molten olivine-basalt aggregates during hot-pressing, *Tectonophysics*, *107*, 207–233, doi:10.1016/0040-1951(84)90252-X.

Faul, U. H., and I. Jackson (2007), Diffusion creep of dry, melt-free olivine, *J. Geophys. Res.*, *112*, B04204, doi:10.1029/2006JB004586.

Gribb, T. T., and R. F. Cooper (2000), The effect of an equilibrated melt phase on the shear creep and attenuation behavior of polycrystalline olivine, *Geophys. Res. Lett.*, *27*(15), 2341–2344, doi:10.1029/2000GL011443.

Hirschmann, M. M. (2010), Partial melt in the oceanic low velocity zone, *Phys. Earth Planet. Inter.*, *179*, 60–71, doi:10.1016/j.pepi.2009.12.003.

Hirth, G., and D. L. Kohlstedt (2003), Viscosity of the upper mantle; the experimentalist's point of view, in *Inside the Subduction Factory*, *Geophys. Monogr. Ser.*, vol. 138, edited by J. M. Eiler, AGU, Washington, D. C.

Jackson, I., U. H. Faul, J. D. Fitz Gerald, and B. H. Tan (2004), Shear wave attenuation and dispersion in melt-bearing olivine polycrystals: 1. Spec-imen fabrication and mechanical testing, *J. Geophys. Res.*, *109*, B06201, doi:10.1029/2003JB002406.

Karato, S., and H. A. Spetzler (1990), Defect microdynamics in minerals and solid-state mechanisms of seismic wave attenuation and velocity eispersion in the mantle, *Rev. Geophys.*, *28*(4), 399–421, doi:10.1029/RG028i004p00399.

Mavko, G. M. (1980), Velocity and attenuation in partially melted rocks, *J. Geophys. Res.*, *85*, 5173–5189, doi:10.1029/JB085iB10p05173.

McCarthy, C., Y. Takei, and T. Hiraga (2011), Experimental study of atten-uation and dispersion over a broad frequency range: 2. The universal scaling of polycrystalline materials, *J. Geophys. Res.*, doi:10.1029/2011JB008384, in press.

Takei, Y. (1998), Constitutive mechanical relations of solid-liquid compo-sites in terms of grain-boundary contiguity, *J. Geophys. Res.*, *103*(B8), 18,183–18,203, doi:10.1029/98JB01489.

Takei, Y. (2000), Acoustic properties of partially molten media studied on a simple binary system with a controllable dihedral angle, *J. Geophys. Res.*, *105*(B7), 16,665–16,682, doi:10.1029/2000JB900124.

Takei, Y. (2001), Stress-induced anisotropy of partially molten media inferred from experimental deformation of a simple binary system under acoustic monitoring, *J. Geophys. Res.*, *106*(B1), 567–588, doi:10.1029/2000JB900361.

Takei, Y., and B. K. Holtzman (2009), Viscous constitutive relations of solid-liquid composites in terms of grain boundary contiguity: 1. Grain boundary diffusion control model, *J. Geophys. Res.*, *114*, B06205, doi:10.1029/2008JB005850.

Takei, Y., K. Fujisawa, and C. McCarthy (2011), Experimental study of attenuation and dispersion over a broad frequency range: 1. The appa-ratus, *J. Geophys. Res.*, doi:10.1029/2011JB008382, in press.

C. McCarthy and Y. Takei, Earthquake Research Institute, University of Tokyo, 1-1-1 Yayoi, Bunkyo-ku, Tokyo 113-0032, Japan. (mccarthy@eri.u-tokyo.ac.jp)